ISSN (Print) 1225-9918
ISSN (Online) 2287-3406
Journal of Life Science 2018 Vol. 28. No. 6. 656~662 DOI : https://doi.org/10.5352/JLS.2018.28.6.656

Protein Engineering of Flavin-containing Monooxygenase from *Corynebacterium glutamicum* for Improved Production of Indigo and Indirubin

Hye Sook Jung[1], Hae Bin Jung[1], Hee Sook Kim[1], Chang Gyeom Kim[2] and Jin Ho Lee[1]*

[1]*School of Food Biotechnology & Nutrition, Kyungsung University, Busan 48434, Korea*
[2]*Department of Bioinformatics & Biosystems, Korea Polytechnics, Gyeonggi-do 13122, Korea*

Received February 21, 2018 / Revised May 29, 2018 / Accepted May 30, 2018

Flavin-containing monooxygenases from *Corynebacterium* (cFMOs) were mutagenized based on homology modeling to develop variants with an enhanced indigoid production capability. The four mutants, F170Y, A210G, A210S, and T326S, which fused to a maltose-binding protein (MBP), were constructed, and their biochemical properties were characterized. Of these, purified MBP-T326S required a higher concentration of exogenous FAD (100 mM) than the wild-type MBP-cFMO for optimal activity and showed a 3.8-fold increase in the k_{cat}/K_m value at 100 μM FAD compared to that of MBP-cFMO at 2 μM FAD. The indole oxygenase activities of MBP-T326S decreased to 63-77% compared to that of the MBP-cFMO In addition, MBP-T326S displayed a very low level of futile NADPH oxidase activities (21-24%) in the absence of a substrate. Mutant proteins except for T326S displayed similar K_m and increased k_{cat}/K_m values compared to the wild-type. MBP-F170Y and -A210S mutants showed elevated indole oxygenase activity higher than 3.1- and 2.9-fold, respectively, in comparison with MBP-cFMO. When indigoid production was carried out in LB broth with 2.5 g/l of tryptophan, *Escherichia coli* expressing cFMO produced 684 mg/l of indigo and 104 mg/l of indirubin, while cells harboring T326S produced 1,040 mg/l of indigo and 112 mg/l of indirubin. The results indicate that the production of indigo was 13% higher when compared to a previous report in which an *E. coli* expressing FMO from *Methylophaga* produced 920 mg/l of indigo. The protein engineering of cFMO based on homology modeling provided a more rational strategy for developing indigoid-producing strains.

Key words : *Corynebacterium glutamicum*, flavin-containing monooxygenase, indigoid, protein engineering, T326S mutant

Introduction

Flavin-containing monooxygenases (FMOs, EC 1.14.13.8) belong to the single-component flavoprotein monooxygenase subfamilies and can oxidize the nucleophilic nitrogen, sulfur, phosphorus, and selenium atoms in a range of structurally diverse compounds [2, 17]. FMOs from mammals are important biocatalysts involved in detoxification of drugs and other xenobiotics such as trimethylamine (TMA), benzydamine, clozapine, itopride, ranitidine, and cimetidine [14]. Meanwhile, the bacterial FMO from *Methylophaga aminisulfidivorans* (mFMO) was known to have the oxygenation activity for *N*-containing amines and *C*-atom in indole [4].

***Corresponding author**
Tel : +82-51-633-4716, Fax : +82-51-622-4986
E-mail : jhlee83@ks.ac.kr

Indigo is one of the oldest blue dyes for the textile industry and currently produced by chemical synthesis [7]. Indirubin and its derivatives have significant therapeutic effects on several human cancers and Alzheimer's disease [5, 6, 11]. To date, several eco-friendly biological approaches have been attempted for production of these indigoids, and high titers of indigo and indirubin were achieved by recombinant cells expressing bacterial FMOs from *M. aminisulfidivorans* and optimization of culture media [9, 10]. We previously identified an FMO from *Corynebacterium glutamicum* (cFMO) with indole oxygenase activity and demonstrated *E. coli* harboring cFMO produced higher concentration of both indigo and indirubin than recombinant cells with other oxygenases [1]. Although bacterial FMOs have a high potential usefulness in biological production of indigo and indirubin, the production performance by them is still much lower than that by chemical synthesis. Therefore, it is necessary to develop mutant FMOs with enhanced catalytic activity and/or indigoid production capability through rational design and mutagenesis.

FMOs require an FAD prosthetic group and an NADPH cofactor [17]. According to crystal structures of yeast and bacterial FMOs, they consist of a large FAD binding domain and a small domain, and the NADPH binding site lies in the crevice between the two domains [3, 8]. In addition, NADPH binding motif sequence that is also involved in diverse substrate binding showed some variations, i.e. GASYA in cFMO, GSSYS in mFMO, and GASSA in *Shizosaccharomyces pombe* FMO [3, 8, 13].

Herein, we engineered three interesting amino residues near FAD and NADPH binding sites based on homology modeling of *Corynebacterium* FMO. Moreover, the indigoid-producing ability of recombinant *E. coli* cells with mutant enzymes was evaluated in terms of production level.

Materials and Methods

Homology modeling

Homology modeling was performed by MODELER version 9.14 [16]. The crystal structure of *Methylophaga* FMO (PDB ID: 2XVH) was used as template for building the homology models [3]. Although the structure of mFMO is consisted of homomultimer, we took only one monomer structure for using as a template since the catalytic active site of that seems not to be affected by intermolecular interaction. Amino acid residues including F170, A210, and T326 interacting with prosthetic groups, FAD and NADPH, by hydrogen bonds and/or hydrophobic interaction were chosen for mutagenesis.

Site-directed mutagenesis

The *Corynebacterium fmo* gene in pMCF14 was used as a template DNA for mutagenesis (Table 1). F170, A210, and T326 residues in cFMO based on homology modeling were mutated by site-directed mutagenesis. To introduce mutation at F170Y, A210G, A201S, and T326S, 5′-and 3′-regions of *fmo* gene were amplified by using primer sets P1-P3 and P4-P2, P1-P5 and P6-P2, P1-P7 and P8-P2, and P1-P9 and P10-P2, respectively (Table 2). The resulting fragments of both regions were combined each other and used for the 2nd round of PCR with P1 and P2, respectively. The final 1.4 kb PCR products with 4 types of mutations were digested with *Eco*RI and *Hin*dIII, ligated with pMAL-c2x/*Eco*RI/*Hin*dIII, and transformed into competent *E. coli* Top10 cells. Constructed plasmids were named as pM-F170Y, pM-A210G, pM-A210S, and pM-T326S, respectively. The introduced mutations were analyzed by DNA sequencing.

Subcloning of mutant cFMOs

To construct plasmids harboring mutant cFMOs without MBP (maltose-binding protein)-tag, the 1.4 kb *fmo*-ORFs of MBP-F170Y, -A210G, -A210S, and -T326S mutants were di-

Table 1. The bacterial strains and plasmids used in this study

Strain or plasmid	Characteristics*	Source or reference
Escherichia coli		
Top10	F⁻*mcr*A Δ(*mrr-hsa*RMS-*mcr*BC) ϕ80*lac*ZΔM15 Δ*lac*X74 *recA1 araD139* Δ*(ara-leu)*7679 *gal*U *gal*K *rps* (Str^R) *end*A1 *nup*G	Invitrogen, USA
W3110	F⁻IN(*rrnD-rrnE*)	This lab.
WCO21	W3110 with pPIO1	This work
WTS326	W3110 with pK-T326S	This work
Plasmids		
pKK223-3	Expression vector with *tac* promoter, Amp^R	This lab.
pPIO1	pKK223-3 derivative; 1.4 kb c*fmo* ORF	Ameria et al. (2015)
pMAL-c2x	Expression vector with *tac* promoter and an ORF of maltose binding protein, Amp^R	New England Biolabs
pMCF14	pMAL-c2x derivative; 1.4 kb c*fmo* ORF	Ameria et al. (2015)
pM-F170Y	pMAL-c2x derivative; 1.4 kb c*fmo* ORF with mutation at T509A (F170Y)	This work
pM-A210G	pMAL-c2x derivative; 1.4 kb c*fmo* ORF with mutation at C629G (A210G)	This work
pM-A210S	pMAL-c2x derivative; 1.4 kb c*fmo* ORF with mutation at G628T (A210S)	This work
pM-T326S	pMAL-c2x derivative; 1.4 kb c*fmo* ORF with mutation at CG977-978GC (T326S)	This work
pK-F170Y	pKK223-3 with c*fmo* with F170Y	This work
pK-A210G	pKK223-3 with c*fmo* with A210G	This work
pK-A210S	pKK223-3 with c*fmo* with A210S	This work
pK-T326S	pKK223-3 with c*fmo* with T326S	This work

*Str^R, streptomycin resistance, Amp^R, ampicillin resistance.

Table 2. Primer lists used in this study

Primer	Sequence (5′-3′)	Restriction enzyme site or comments
P1	CCCGGAATTCATGGAGATGGTTATGAAGAA	*Eco*RI
P2	CCCCAAGCTTTTAGGCTTTATCGCGGACTT	*Hin*dIII
P3	GGGACGTTCGGGAAGCTGTAGTGTCCAGCGCCAACAA	F170Y-R
P4	TTGTTGGCGCTGGACACTACAGCTTCCCGAACGTCCC	F170Y-F
P5	CTTCCGCAGAATAACTTCCACCAATCAGCAAAATA	A210G-R
P6	TATTTTGCTGATTGGTGGAAGTTATTCTGCGGAAG	A210G-F
P7	TTCCGCAGAATAACTTGAACCAATCAGCAAAATAT	A210S-R
P8	ATATTTTGCTGATTGGTTCAAGTTATTCTGCGGAA	A210S-F
P9	AGCATCAAACATGTTGAAGCTCAGCCACTGATCCTGAG	T326S-R
P10	CTCAGGATCAGTGGCTGAGCTTCAACATGTTTGATGCT	T326S-F

gested with *Eco*RI and *Hin*dIII, ligated with *Eco*RI/*Hin*dIII-cleaved pKK223-3, respectively, and yielded plasmids pK-F170Y, pK-A210G, pK-A210S, and pK-T326S (Table 1).

Expression and purification of mutant MBP-cFMOs

E. coli Top10 cells expressing mutant MBP-cFMOs were cultured at 28℃ in LB (10 g/l tryptone, 5 g/l yeast extract, and 10 g/l NaCl) broth with shaking at 180 rpm. Expression of mutant MBP-cFMOs was induced by adding 0.1 mM IPTG into culture broth when cell OD_{600nm} reached to 0.5-0.6. The purification of mutant MBP-cFMOs was performed according to previously described method [1]. The purified enzymes were analyzed by SDS-PAGE and protein concentrations were measured by the Bradford method (Bio-Rad) with bovine serum albumin as the standard.

Enzyme assay

To investigate biochemical properties of mutant cFMOs, NADPH oxidase activity was measured according to previously reported method [1] with TMA as a substrate. Futile NADPH oxidase activity was determined in the absence of substrate at the same assay condition. Indole oxygenase activity was determined at 5 mM indole [1]. All enzyme assays described above were performed in triplicate experiments.

Production of indigoid and analyses of indigo, indirubin, and tryptophan

Production of indigo and indirubin was performed in LB medium containing 2.5 g/l of tryptophan with IPTG induction in a shaking incubator at 32℃ for 48 hr using recombinant *E. coli* W3110 expressing mutant cFMOs. The amounts of indigo, indirubin, and tryptophan were analyzed by HPLC [12]. All cell cultures were performed in triplicate experiments.

Results and Discussion

Construction of mutant MBP-cFMOs based on rational design

Although the structure of cFMO has not been resolved so far, we could build a reliable 3D structure model by homology modeling because its sequence has a quite high identity with mFMO (56%), of which structure data were published (PDB ID: 2XVE) [3]. The model of cFMO is superimposed very well with crystal structure of mFMO, and the RMS (root mean square) of the overlapped structures was only 0.063 Å. Under the visual inspection of the cFMO model, three residues which are located closely enough to cofactors and substrates at the catalytic site were chosen (Fig. 1). First, the benzyl side chain of F170 was found to be located at a distance of 3.4 Å and 3.6 Å from the hydroxyl group of C-2 in the ribitol of FAD and that of C-3 in the nicotinamide ribose of NADPH, respectively, which seems to affect affinity between cFMO and cofactors. Second, in order to accommodate the cofactor NADPH, A210 in GASYA loop region (209-213 amino acid residues) which is thought to an important role for NADPH binding was picked and replaced to glycine or serine. Third, T326 is located closer than 3.5 Å from isoalloxazine ring of FAD and may be had an impact on the interaction with FAD. Based on these ideas, four MBP-cFMO mutants F170Y, A210G, A210S, and T326S were constructed in *E. coli* by site-directed mutagenesis.

Biochemical properties of mutant MBP-cFMOs

In order to characterize biochemical properties of mutant

Table 3. Kinetic parameters for mutant MBP-cFMOs from *C. glutamicum* using TMA as the substrate

Enzyme*	K_m (mM)	V_{max} (nmol/min/mg protein)	k_{cat} (/min)	k_{cat}/K_m (/min/mM)
MBP-cFMO	0.575	1608.0	156.1	271.3
MBP-F170Y	0.531	2839.9	275.7	518.8
MBP-A210G	0.441	1377.5	133.7	303.0
MBP-A210S	0.445	1936.3	188.0	422.6
MBP-T326S	0.237	462.9	44.9	189.9
MBP-T326S†	0.035	376.2	36.5	1034.5

*Kinetic parameters for wild-type and mutant MBP-cFMOs were determined at 2 μM FAD.
† Kinetic parameters for mutant MBP-T326S were determined at 100 μM FAD.

enzymes, kinetic studies of the purified four mutants as well as wild-type MBP-cFMO were performed using TMA as a substrate (Table 3). Mutant proteins except for T326S displayed similar K_m and increased k_{cat}/K_m values compared to the wild-type. In particular, MBP-F170Y had 1.9-fold higher k_{cat}/K_m than control protein. When MBP-cFMOs were purified by using amylose resin, most purified mutants showed yellow color, but not MBP-T326S protein in which the binding affinity for FAD seemed to be greatly decreased due to the structural change. Wild-type and other mutants required 2 μM of FAD for optimal activity [1], while T326S mutant required 100 μM of exogenous FAD (data not shown). T326S had 16.4- and 3.8-folds increased substrate affinity and k_{cat}/K_m for TMA, respectively, at 100 μM FAD compared to those of MBP-cFMO at 2 μM FAD (Table 3). The indole oxygenase activity was also determined using wild-type and mutant MBP-cFMO proteins (Fig. 2). F170Y and A210S mutants showed elevated indoxyl production activity more than 3.1- and 2.9-folds, respectively, in comparison to MBP- cFMO, whereas T326S displayed a decreased activity regardless of FAD concentrations. According to the proposed catalytic scheme for mFMO [3], NADPH reduces oxidized FAD bound to mFMO, which interacts with an oxygen molecule and is converted to peroxyFAD and $NADP^+$ in the reductive half of the reaction. When substrate indole is present, peroxyFAD returns to the oxidized form with releasing indoxy and water molecules. However, in the absence of substrate, peroxyFAD might be slowly oxidized and released H_2O_2, which is called as futile NADPH oxidase activity. In this study, wild MBP-cFMO and most mutants showed similar futile activities in the absence of substrate, whereas T326S at both 2 μM and 100 μM FAD had significantly decreased futile activity compared to the wild-type (Fig. 3).

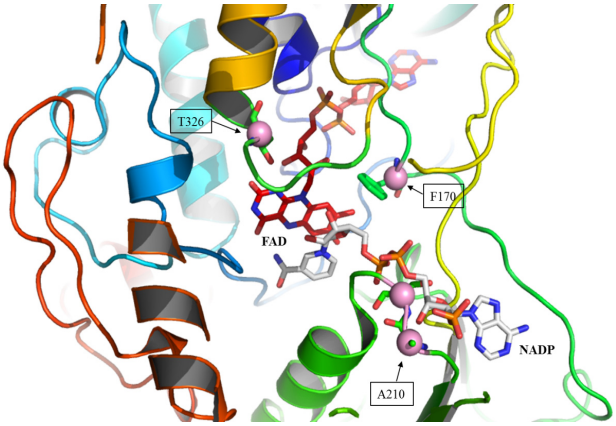

Fig. 1. The detailed 3D structure model around catalytic active site in cFMO. FAD and NADP are represented by red and white colors, respectively, and three mutation points are shown by balls and sticks, which are F170, A210, and T326.

Effect of mutant cFMOs on indigo and indirubin production

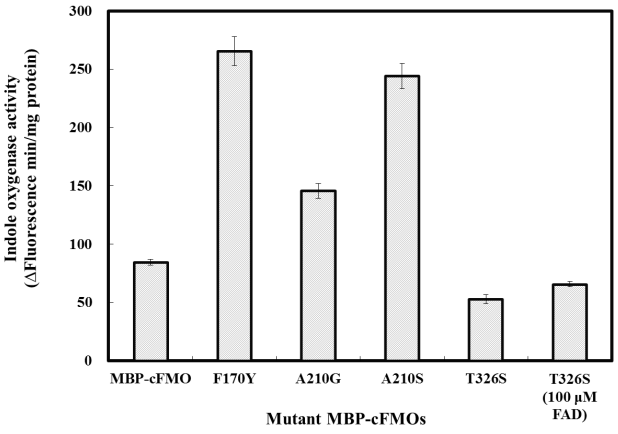

Fig. 2. Indole oxygenase activity of mutant MBP-cFMOs. Indole oxygenase activity of mutant MBP-cFMOs was measured by the fluorescence of indoxyl in the presence of 5 mM indole and 2 μM FAD except MBP-T326S shown in the rightmost bar in which the activity was determined at 100 μM FAD.

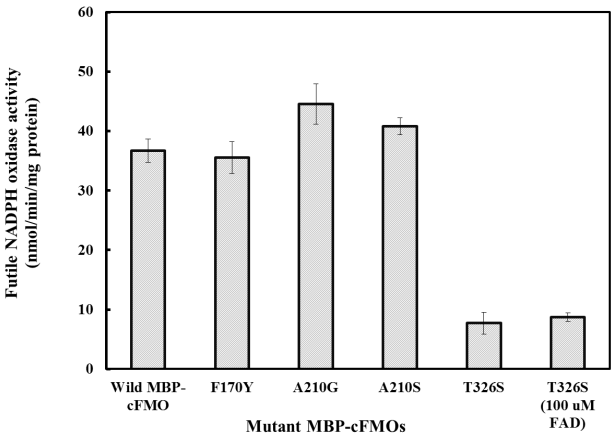

Fig. 3. Futile NADHP oxidase activity of mutant MBP-cFMOs. Futile NADHP oxidase activity of mutant MBP-cFMOs was determined at 2 μM FAD in the absence of substrate except for MBP-T326S shown in the rightmost bar in which the activity was determined at 100 μM FAD.

Because the production of indigo and indirubin in *E. coli* cells harboring wild-type or mutant cFMOs fused to MBP was poor, the production performance of indigoid was evaluated by using *E. coli* with wild-type or mutant cFMOs without MBP-tag in flask culture. Although the purified MBP-F170Y and MBP-A210S mutants showed higher indole oxygenase activity, indigoid production was not increased by introduction of the mutant F170Y or A210S into *E. coli* compared with WCO21 (Fig. 4A, Fig. 4B). When *E. coli* expressing A210G was cultured for 48 h, less than 20 mg/l of indigo and indirubin were obtained with little consumption of tryptophan (Fig. 4). Recombinant *E. coli* WTS326 harboring pK-T326S produced 1,040 mg/l of indigo and 112 mg/l of indirubin with consuming 2.44 g/l of tryptophan, which were 52% and 8%, respectively, higher than those obtained with the control strain expressing cFMO (Fig. 4). This result indicated that indigo titer was increased about 13% compared to the previous report in which the highest level, up to date, was 920 mg/l in *E. coli* expressing mFMO [10]. Since FMOs requires NADPH for a reducing power, an efficient supply or strong regeneration of NADPH pool is crucial for oxygenation of indole [15]. Even though MBP-T326S showed 63-77% indole oxygenase activities compared to MBP-cFMO, low levels of the futile NADPH oxidase activities (21-24%) in MBP-T326S would lead to save the NADPH pool in cells, resulting in higher production of indigoid. Thus, our result suggests that a decreased futile NADPH oxidase activity plays an important role in WTS326 strain for production of indigoid. A previous result regarding indigo production system also demonstrated that the expression of glucose dehydrogenase in indigo-producing *E. coli* led to the efficient regeneration of NADPH and the improved production of

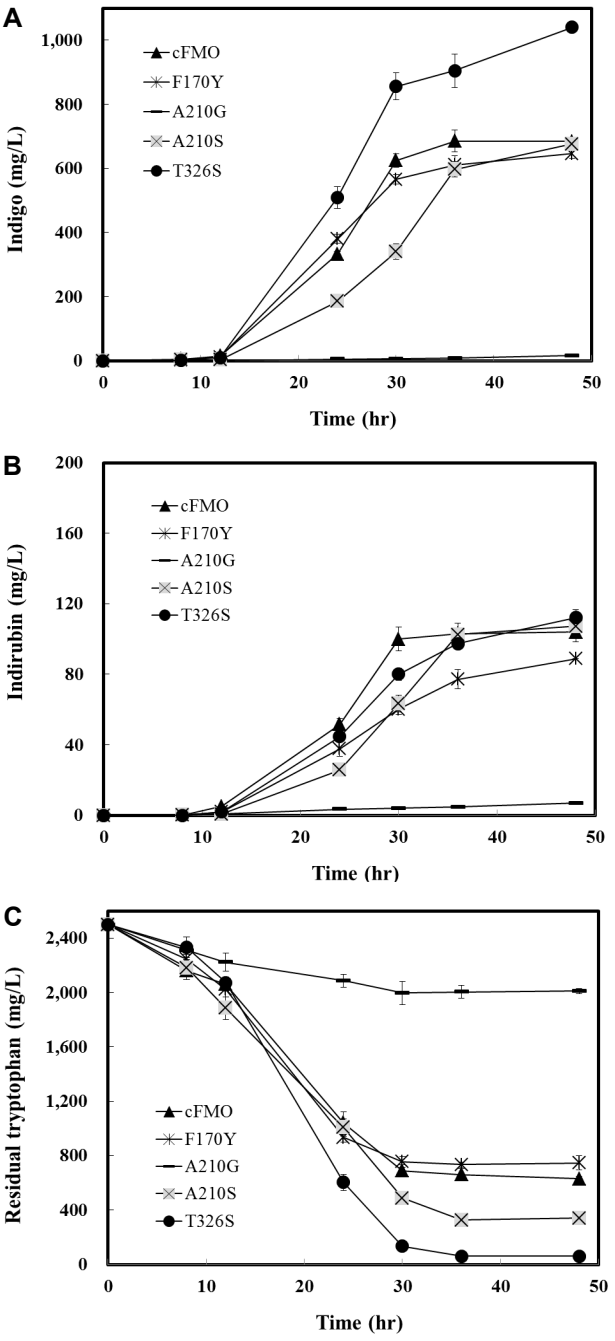

Fig. 4. Production of indigo and indirubin by recombinant *E. coli* cells expressing mutant FMOs. (A) and (B) show the production level of indigo and indirubin, respectively, by *E. coli* cells with mutant FMOs. (C) shows the tryptophan concentration during cultivation time. Recombinant strains were cultured in LB medium with 2.5 g/l of tryptophan for 48 hr at 32℃. Indigo, indirubin, and tryptophan concentrations were determined by HPLC analyses.

indigo [15].

Molecular modeling of T326S mutant

Among several mutants, MBP-T326S exhibited a decreased affinity for FAD and a low futile NADPH oxidase activity compared to control MBP-cFMO (Table 3, Fig. 3). According to 3D structure model of the wild type cFMO, the hydrophobic methyl group of T326 pushed out the hydrophilic carbonyl group of Q323 and, as a result, the carbon backbone of FAD could be stabilized in the hydrophobic environment formed by the methyl group of threonine at residue 326 and the γ-carbon of glutamine at residue 323. In addition, FAD may be stabilized by hydrogen bond between >C=O group in wild-type Q323 and -OH group of the 2′-carbon attached to a flavin ring of FAD (Fig. 5). In T326S mutant, we could predict that most of residues around S326 are not changed in their conformation except the neighbor residue Q323 and F327 which seem to change the rotamer conformation. The absence of methyl group in S326 could make a room for accommodating the carbonyl group of Q323 and move in near to S326. When the hydrophilic residue of Q323 directs to the hydrophobic carbon backbone of FAD, FAD could not get much favorable interaction with T326S compared to the wild-type. Furthermore, although the distance between the carbonyl group of Q323 and the hydroxyl group of 2′-carbon of flavin in T326S mutant is close to 2.9 Å, the angle between them seems to be not proper for strong hydrogen bond. In vitro assay regarding requirement of high concentrations of FAD up to 100 μM for MBP-T326S activity is presumably correlated with molecular modeling of T326S, which suggests the T326S mutant shows significant decreased affinity for FAD in comparison to the wild-type due to the absence of methyl group in S326 and improper hydrogen bond between Q323 and FAD. But, the correlation between T326S mutation and the low futile NADPH oxidase activity is a future task to be studied.

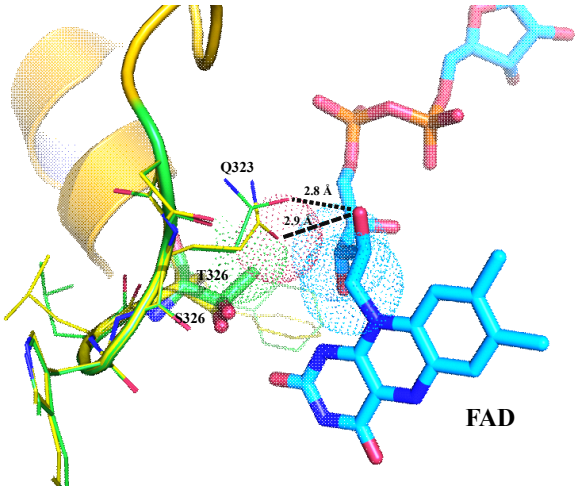

Fig. 5. The detailed overlapped 3D structure model around T326, S326, and Q323 residues in cFMO and T326S. A loop of wild type cFMO is shown in green and that of T326S mutant is shown in yellow. Dotted spheres represent Van der Waals radii for atoms.

Acknowledgement

This research was supported by Basic Science Research Program through the National Research Foundation of Korea (NRF) funded by the Ministry of Education, Science and Technology (NRF-2012R1A1A2007229).

References

1. America, S. P. L., Jung, H. S., Kim, H. S., Han, S. S., Kim, H. S. and Lee, J. H. 2015. Characterization of a flavin-containing monooxygenase from *Corynebacterium glutamicum* and its application to production of indigo and indirubin. *Biotechnol. Lett.* **37**, 1637-1644.
2. Cashman, J. R. 2005. Some distinctions between flavin-containing and cytochrome P450 monooxygenases. *Biochem. Biophys. Res. Commun.* **338**, 599-604.
3. Cho, H. J., Cho, H. Y., Kim, K. J., Kim, M. H., Kim, S. W. and Kang, B. S. 2011. Structural and functional analysis of bacterial flavin-containing monooxygenase reveals its ping-pong-type reaction mechanism. *J. Struct. Biol.* **175**, 39-48.
4. Choi, H. S., Kim, J. K., Cho, E. H., Kim, Y. C., Kim, J. I. and Kim, S. W. 2003. A novel flavin-containing monooxygenase from *Methylophaga* sp. strain SK1 and its indigo synthesis in *Escherichia coli*. *Biochem. Biophys. Res. Commun.* **306**, 930-936.
5. Ding, Y., Qiao, A. and Fan, G. H. 2010. Indirubin-3′-monoxime rescues spatial memory deficits and attenuates beta-amyloid-associated neuropathology in a mouse model of Alzheimer's disease. *Neurobiol. Dis.* **39**, 156-168.
6. Eisenbrand, G., Hippe, F., Jakobs, S. and Muehlbeyer, S. 2004. Molecular mechanisms of indirubin and its derivatives: novel anticancer molecules with their origin in traditional Chinese phytomedicine. *J. Cancer Res. Clin. Oncol.* **130**, 627-635.
7. Ensley, B. D., Ratzkin, B. J., Osslund, T. D., Simon, M. J., Wackett, L. P. and Gibson, D. T. 1983. Expression of naphthalene oxidation genes in *Escherichia coli* results in the biosynthesis of indigo. *Science* **222**, 167-169.
8. Eswaramoorthy, S., Bonanno, J. B., Burley, S. K. and Swaminathan, S. 2006. Mechanism of action of a flavin-containing monooxygenase. *Proc. Natl. Acad. Sci. USA.* **103**, 9832-9837.
9. Han, G. H., Gim, G. H., Kim, W., Seo, S. I. and Kim, S. W. 2012. Enhanced indirubin production in recombinant *Escher-*

ichia coli harboring a flavin-containing monooxygenase gene by cysteine supplementation. *J. Biotechnol*. **164**, 179-187.
10. Han, G. H., Shin, H. J. and Kim, S. W. 2008. Optimization of bio-indigo production by recombinant *E. coli* harboring *fmo* gene. *Enzyme Microb. Technol*. **42**, 617-623.
11. Hoessel, R., Leclerc, S., Endicott, J. A., Nobel, M. E., Lawrie, A., Tunnah, P., Leost, M., Damiens, E., Marie, D., Marko, D., Niederberger, E., Tang, W., Eisenbrand, G. and Meijer, L. 1999. Indirubin, the active constituent of a Chinese antileukaemia medicine, inhibits cyclin-dependent kinases. *Nat. Cell Biol*. **1**, 60-67.
12. Kang, M. S. and Lee, J. H. 2009. Cloning and expression of indole oxygenase gene derived from *Rhodococcus* sp. RHA1. *Kor. J. Microbiol. Biotechnol*. **37**, 197-203.
13. Kleiger, G. and Eisenberg, D. 2002. GXXXG and GXXXA motifs stabilize FAD and NAD(P)-binding Rossmann folds through C^{α}–H···O hydrogen bonds and van der Waals interactions. *J. Mol. Biol*. **323**, 69-76.
14. Krueger, S. K. and Williams, D. E. 2005. Mammalian flavin-containing monooxygenases: structure/function, genetic polymorphisms and role in drug metabolism. *Pharmacol. Ther*. **106**, 357-387.
15. Lu, Y. and Mei, L. 2007. Co-expression of P450 BM3 and glucose dehydrogenase by recombinant *Escherichia coli* and its application in an NADPH-dependent indigo production system. *J. Ind. Microbiol. Biotechnol*. **34**, 247-253.
16. Šali, A. and Blundell, T. L. 1993. Comparative protein modelling by satisfaction of spatial restraints. *J. Mol. Biol*. **234**, 779-815.
17. Van Berkel, W. J., Kamerbeek, N. M. and Fraaije, M. W. 2006. Flavoprotein monooxygenases, a diverse class of oxidative biocatalysts. *J. Biotechnol*. **124**, 670-689.

초록 : 인디고와 인디루빈의 생산을 증대하기 위한 플라빈-함유 모노옥시게나제의 단백질공학

정혜숙[1] · 정혜빈[1] · 김희숙[1] · 김창겸[2] · 이진호[1]*
([1]경성대학교 식품응용공학부, [2]한국폴리텍대학 생명정보시스템과)

향상된 인디고이드 생산능력을 갖는 코리네박테리움 유래의 변이 플라빈-함유 모노옥시게나제(cFMO)를 개발하기 위하여, cFMO 효소의 상동성모델을 이용하여 말토오스-결합단백질(MBP)과 융합된 4가지 변이체(F170Y, A210G, A210S, T326S)를 제작하고 그 생화학적 특징을 밝혔다. 정제된 MBP-T326S는 최적 활성을 위하여 야생형보다 고농도의 FAD (100 μM)를 요구하며, 100 μM의 FAD 첨가조건에서 k_{cat}/K_m이 3.8배 증가되었다. 인돌 옥시게나제 활성은 야생형의 63-77%를 나타냈다. MBP-T326S는 기질이 존재하지 않을 경우 쓸모없는 NADPH 산화효소 활성이 매우 낮은 수준을 보여주었다(21-24%). T326S이외의 변이 단백질들은 야생형에 비하여 K_m은 비슷하며 k_{cat}/K_m은 증가하였다. MBP-F170Y와 -A210S 변이단백질은 인돌 옥시게나제 활성이 각각 3.1배, 2.9배 증가하였다. 2.5 g/l의 트립토판을 함유한 LB배지에서 인디고이드 생산을 시험했을 때, 야생형 cFMO를 함유한 대장균은 684 mg/l의 인디고와 104 mg/l의 인디루빈을 생산한 반면, T326S를 함유한 세포는 1,040 mg/l의 인디고와 112 mg/l의 인디루빈을 생산하였다. 이전의 결과인 *Methylophaga* 유래의 FMO를 발현하는 대장균에서 가장 높은 수준인 920 mg/l의 인디고를 생산한 것과 비교하면, 본 연구결과는 인디고 생산이 13% 높은 수준이였다. 상동성 모델링에 기반한 cFMO의 단백질공학은 인디고이드 생산균을 개발하는데 보다 더 논리적인 전략을 제시하였다.